

FINAL REPORT FOR "LAKE TAHOE ASIAN CLAM SURVEY PROJECT" TO THE LAHONTAN REGIONAL
WATER QUALITY CONTROL BOARD

Grant Agreement 09-633-550

Grantee: The Regents of the University of California, on behalf of its Davis Campus

P.I. Geoff Schladow, PhD, Director of Tahoe Environmental Research Center

Table of Contents

1.0	Introduction
2.0	Methods
2.1	<i>UBC-Gavia: An Autonomous Underwater Vehicle</i>
2.2	<i>Mission Design</i>
2.3	<i>Image Algorithm</i>
2.4	<i>Algorithm Calibration</i>
3.0	Detection Results
3.1	<i>Raw Data Results</i>
3.2	<i>Groundtruthing Surveys</i>
3.3	<i>Across Shore Transects</i>
4.0	Optical backscatter
4.1	<i>Temperature and Conductivity Results</i>
4.2	<i>Chlorophyll a, CDOM and turbidity Results</i>
5.0	Correlation between filamentous algae and Asian clam presence
6.0	Other observations
7.0	Conclusions
8.0	Acknowledgements
9.0	References

1.0 Introduction

The discovery of high-density populations of the invasive bivalve Asian clam (*Corbicula fluminea*) in Lake Tahoe in 2008 prompted an immediate response by management agencies and scientific institutions of the basin. The Asian clam working group (ACWG) formed in 2008 and began carrying out policy driven ecological research in the lake with the following objectives: (1) to characterize the extent of the new Asian clam invasion in Lake Tahoe; (2) to understand impacts of Asian clam on native ecology and water quality; and, (3) to experiment with potential control or management strategies to understand if control of this species is feasible. During the summer and fall periods of 2008, quantitative observations of the nearshore zone by researchers at the University of California Davis (UCD) and the University of Nevada Reno (UNR) suggested that heterogeneous populations of Asian clam were present in variable densities in portions of the southeastern quadrant of the lake. The research team used a highly quantitative, yet labor intensive, “brute force” methodology (benthic grab samplers) to characterize Asian clam abundance along multiple vertical transects in Zephyr Cove, Marla Bay, Nevada Beach, Timber Cove, and Pope Beach (Figure 1). This method is a classically used technique in benthic ecology and was beneficial to define benthic macroinvertebrate communities in specific regions as well as to quantify impacts that Asian clam are having on native communities. However, benthic grab sampling is not ideal for use in characterizing the range or extent of macroinvertebrate populations due to the high level of field and laboratory effort and the prohibitively large size of Lake Tahoe relative to the size of ‘satellite’ populations that are outside the boundaries of the primary distribution. In order to characterize the extent of the Asian clam population in Lake Tahoe in an efficient manner, the ability to rapidly image the bottom of the lake to detect Asian clam shell matter was necessary. Autonomous underwater vehicles

(AUVs) are frequently utilized in applications for limnological habitat assessment, hydrography, bathymetric surveys, archeology, wreck finding and mapping and bottom type classifications because of its ease of deployment and efficient survey abilities (e.g. Moline et al., 2007; Singh et al., 2004). An AUV was brought to Lake Tahoe in January 2009 to test its ability to detect Asian clam shell matter. It was determined that the collected images using this technology would be well suited for the purposes of a rapid, whole lake survey.

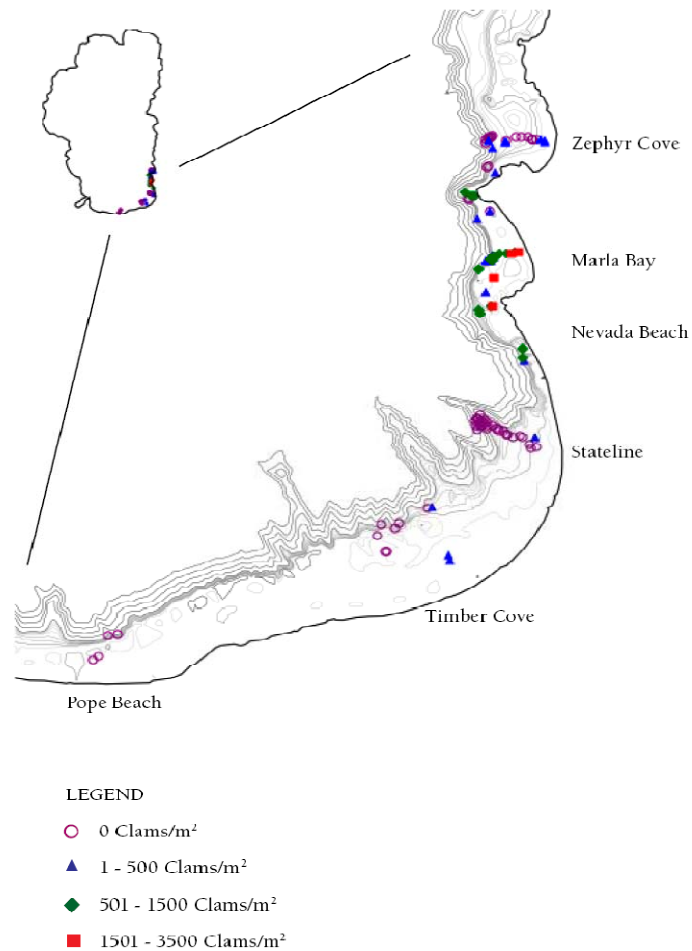


Figure 1. Locations and densities of Asian clam populations based on benthic grab sample transects as measured in 2008. A useful method for localized quantitative benthic community characterization.

The need to characterize the Asian clam population in Lake Tahoe was motivated by two factors;

(1) management needs – an understanding of the extent of the infestation will define control

programs, and (2) the understanding of the relationship between observed filamentous algal blooms in 2008 and 2009 and the presence of Asian clam in the littoral zone.

The experimental use of an autonomous underwater vehicle (AUV) to survey for Asian clam was warranted because of its ability to cover a large amount of area in a short amount of time (i.e. full lake survey at a specified isobath in less than 2 weeks). The proposed mechanism for Asian clam detection by AUV was to collect high-resolution imagery of the lake bottom and to characterize the amount of shell matter in each region based on the amount of whiteness on the bottom of the lake in each frame and then correcting for vehicle altitude. The high-resolution imagery also allowed for the observation of other benthic characteristics such as the detection of filamentous algae, aquatic macrophytes and other effects of the lake bottom. In addition, the scientific payload of the AUV allowed for the measurements of conductivity, temperature, turbidity, chlorophyll *a*, and colored dissolved organic matter (CDOM). This allows for lateral variability in these factors to be quantified around the lake and observe correlations with clam population distributions. After the AUV deployment, the science team then image truthed and ground truthed the image detections of Asian clam shell material to confirm the presence/absence of Asian clam and to also correlate the relationship between the *UBC-Gavia* detections with live population density.

The lake survey was conducted over a two-week period in August 2009 and the first results from the survey were presented to the ACWG as well as the Lake Tahoe AIS Coordination Committee (LTAISCC) in September 2009. Since that time, the data processing has been refined and is presented herein.

2.0 Methods

This work represented collaboration between the Universities of California Davis, Nevada Reno, British Columbia and Delaware. The survey employed the use of *UBC-Gavia*, an autonomous underwater vehicle (AUV) owned and operated by the Environmental Fluid Mechanics group at UBC, to collect benthic imagery following transects running along-shore, and subsequently across-shore, at specific locations where clam matter densities were determined to be elevated. Concurrent water column measurements were made with an optical backscatter sensor and a high-resolution conductivity-temperature-depth (CTD) profiler.

2.1 UBC-Gavia: An Autonomous Underwater Vehicle

Figure 2 provides a schematic of *UBC-Gavia* in its base standard configuration indicating the primary vehicle modules along with the associated onboard scientific and navigational sensors. Due to the vehicle modularity, sections can be interchanged depending on the mission requirements and are joined along an Ethernet bus that the control software will automatically detect in a 'plug-and-play' fashion. For the deployment in Lake Tahoe, a phase-measuring swath bathymetry (GeoSwathTM) sonar unit and an inertial navigational (INS) unit were used in replacement of the Acoustic Doppler Current Profiler (ADCP) unit as the INS had a 1200 kHz RDI Doppler Velocity Log (DVL) permanently joined to it. The INS was required to provide high precision positional data in order that each of the collected images could be georeferenced in postprocessing analysis. In addition, the low position drift (maximum of ~ 0.5% by distance traveled) of this unit, allowed the vehicle to stay submerged for greater periods of time before surfacing for new GPS fixes. In the indicated design, as configured for freshwater operation, the vehicle is approximately 2.4 m in length, 0.2 m in diameter and 55 kg dry weight in air. This required that the ballasting be readjusted each time the vehicle was reconfigured. The maximum

velocity of *UBC-Gavia* is 3.0 m s^{-1} ; however, typical cruising and diving speeds are 1.2 and 2.0 m s^{-1} respectively. The slower cruising speed was selected to prevent blurring in the collected images.

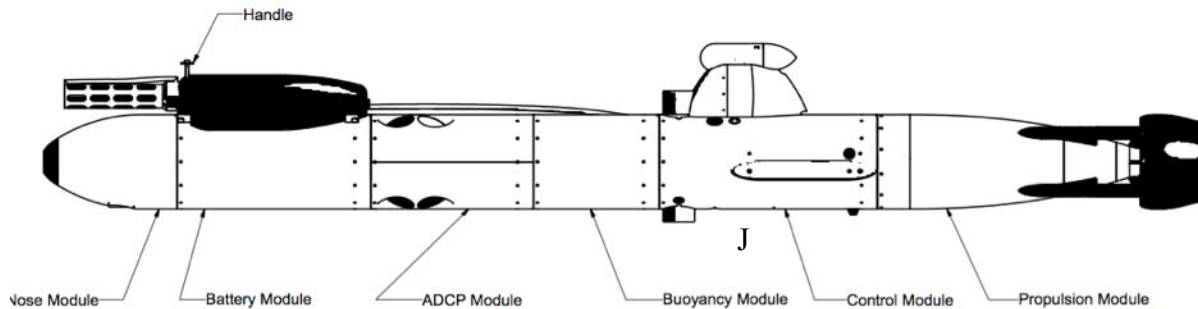


Figure 2. Schematic of *UBC-Gavia*. Each of the on-board modules are indicated directly in the figure and as are the major scientific components: A - Forward collision-avoidance sonar; B - SBE49 FastCat CTD; C - High resolution digital camera; D - Upward looking 1200kHz RDI ADCP; E - Downward looking 1200 kHz RDI ADCP with DVL functionality; F - Wetlabs three wavelength backscatter sensor; G - Imagenex 220/990 kHz sidescan sonar; H - Acoustic modem; I - Communications tower; and, J – position of strobe light associated with camera (not shown in schematic).

With all onboard instrumentation operating, the full battery life is 6 – 8 hours. However, due to technical difficulties with the internal control circuit, the battery life only lasted between 3 – 4 hours. At the previously mentioned typical cruising speed, this gives an operating range of approximately 13 – 17 km. For these missions, one of the challenges faced was the memory storage on the camera flash drive and the ~ 60 minute download time required after each mission effectively reducing data collection time to 2 – 3 hours. The power management strategy that was undertaken was to have a spare battery module on board that would be swapped out midway through each deployment.

Dead-reckoning, or estimating position from predicted speeds and elapsed time with no known geo-referenced point, is calculated using directional information from the internal magneto-

inductive electronic compass and tilt sensors, depth information from the pressure sensor and speed information based on the calculated speed based on the propeller speed (much less accurate) or the measured velocity from the downward facing 1200 kHz, RDI Workhorse Navigator, ADCP. The ADCP provides reliable navigational data when the Doppler velocity log (DVL) is within range of bottom tracking (<30 m). In replacement of this unit, the INS is equipped with a similar downwards-pointed 1200 kHz DVL unit that reduces the navigational error accumulation rate and tracks the bottom with the same accuracy. The AUV has a navigational error propagation algorithm that will halt a mission if an adjustable threshold value is attained. The onboard scientific payload includes a high-resolution digital camera with a 1 W high-intensity LED strobe light system, a Seabird SBE 49TM Conductivity-Temperature-Depth (CTD) recorder, an ImagenexTM dual-frequency (220/990) sidescan sonar, and a WET Labs BB3TM scattering meter. The scattering meter records three different frequencies that are converted to turbidity, chlorophyll-*a* and CDOM. All of the data streams are written to flash drive in raw form. Post-processing then enables the user to standardize the dataset to one measurement frequency and correct for the AUV attitude (e.g. pitch, roll, yaw) and height above the bottom.

2.2 Mission Design

Two mission types were run during the field survey: (1) along-shore transects following the 5 m isobath, and (2) across-shore (inshore-offshore) transects at selected sites based on the processed data from the first survey. The location for each of the nightly missions is shown in Figure 3 and it is shown that the vehicle covered nearly 80 % of the shoreline. The remaining 20% of the shoreline was not surveyed with the AUV because it was determined to be inhospitable habitat for Asian clam (sheer walls or boulder) or because a detailed scuba survey for Asian clam would

be carried out in the weeks following the AUV survey (i.e., Emerald Bay). The littoral region of Lake Tahoe is characterized by a shallow shelf that shoals from 0 – 10 m before dropping off steeply (between 10 – 30° slopes) and running down to full lake depth, with additional steep gullies running perpendicular to the shoreline. It is not possible to program *UBC-Gavia* to follow a contour directly, as this would require adaptive mission planning based on altitude information, which is currently unavailable on most AUVs (Bennett and Leonard, 2000). For this reason, the mission planner requires detailed knowledge of the near-shore bathymetry. Multibeam data of Lake Tahoe, freely available from the Scripps Institution of Oceanography Visualization Center (<http://siovizcenter.ucsd.edu/library/>), was visualized in Fledermaus (produced by IVS 3D) and used to generate contours that were exported into the mission planning software (Figure 4).

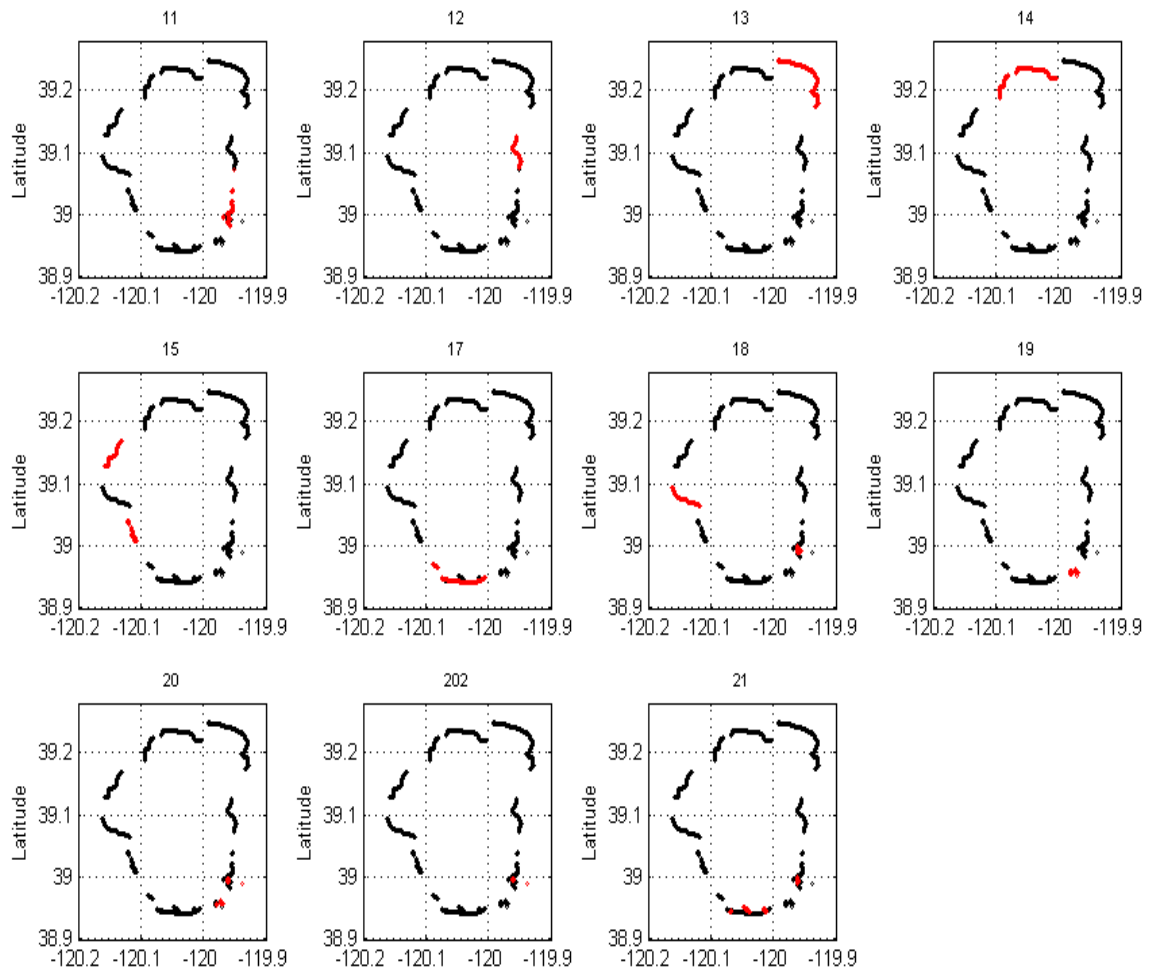


Figure 3. Eleven missions conducted from August 09 to August 22 2010; each mission is highlighted in red. Missions were conducted at night to avoid recreational boating and to optimize image quality by minimizing light interference during the day time and distances ranged from 13 – 17 km.

The strategy that was used was to get the AUV to follow short line segments at a preprogrammed constant altitude of 2.3 m off the bottom (selected for best images). Once the mission was planned, the mission tracks were exported to Google Earth for confirmation that no subsurface or surface obstructions would be encountered (e.g. piers, rock piles, boat launches, etc.).

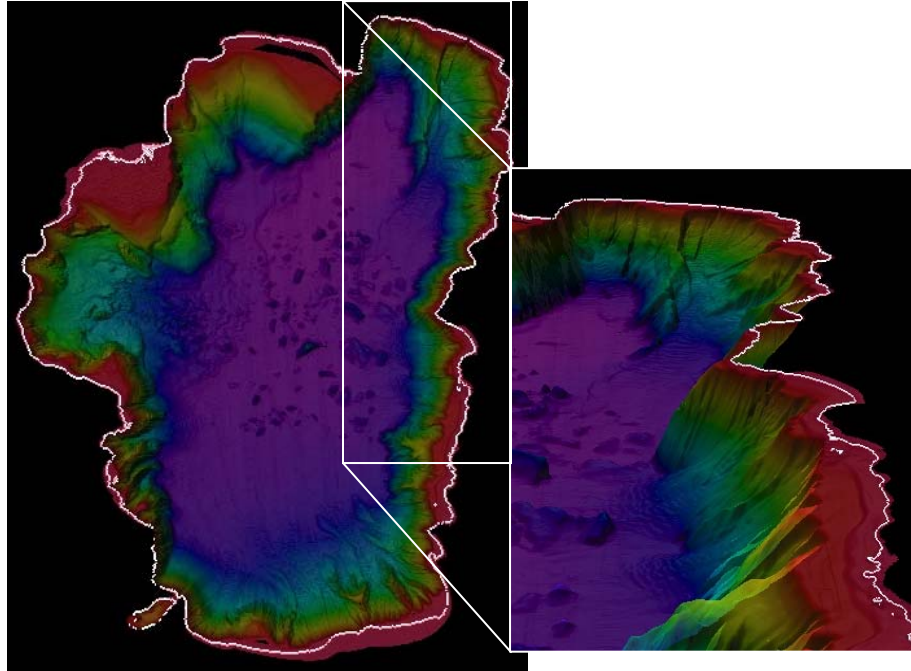


Figure 4: Multibeam data of Lake Tahoe with 5 m contour labeled in main image and then detailed view provides a close up perspective of the shoreline complexity along the east shore north of Zephyr Cove.

Collecting images on the across-shore transects proved to be extremely difficult due to the encountered slopes. Ideally images are collected on slopes less than 10° , which is characteristic of the near-shore littoral zone but the slopes begin to drop off quickly at the shelf break to values greater than 20° . Using the same software package as before, it is possible to find the regions of steep slope gradients (Figure 5). This was then used to plan missions accordingly to try and minimize the flight plans where the AUV would be in regions of steep gradients. In addition, this was also used to choose transects of lesser slopes to keep the vehicle in range of the bottom (it has difficulty tracking slopes $> 15^\circ$) as much as possible. All missions were run at night for four reasons: (1) to standardize light levels at different depths to aid in the high resolution imaging of the lake bottom; (2) to minimize disturbance from recreational boating during the survey; (3) the

generally calmer conditions at night; and, (4) to be able to track the strobe light of the camera (and thus locate the AUV) as it traveled through the water column.

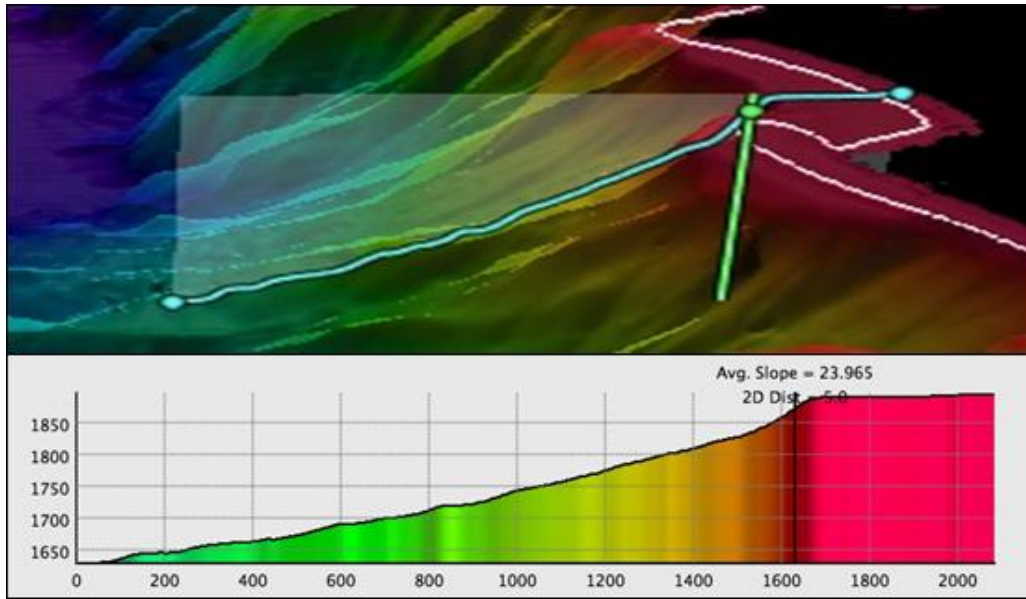


Figure 5. Illustration of the slope characteristics using Fledermaus (visualization software), with the green line in the 3D visualization being reflected in the black vertical line and the slope profile being shown by the cyan line (units of the lower panel are in m a.s.l. – vertical axis and m along line – horizontal axis).

2.3 *Image Algorithm*

Images were collected at a sample frequency of 4 Hz (4 frames per second), which translates into greater than 500,000 images being collected during the field deployment. This means that an analysis program needed to be written to automate the analysis of the photos. This was originally written in Matlab 2007b but could be easily ported into any programming language for future applications. When the clams die, the shells will generally open and show up as white on the lake bottom and easily viewable in the collected images. It was decided to use the shells of dead clams as a proxy for live clams, as they were much easier for detection in the images than the live populations were, as these are generally partially buried beneath the surface. In the first

iteration of the analysis, the program looked simply for those pixels in the image that exceeded a certain color intensity threshold (black equals 0 and white is the sum of the RGB layers equal to 768) that was to be calibrated to eliminate any reflectance from the bottom sediment material. As a result of different ground conditions, it was shown that this method was unsuccessful as there were too many false detects even post-calibration (Figure 6a). The strategy that was adopted instead was to perform a histogram analysis on each frame collected by the AUV by converting this frame (600 x 800 pixels) to its numerical equivalent and then constructing a histogram of this data. Detects based on each pixel would then be counted by either considering a 95 % confidence interval of the deviation away from the mode ('Mode Detects' – green circles in Figure 6b) and the mean ('Mean Detects' – red circles in Figure 6b). As shown, this provided significantly better results than the initial method and was used in the rest of the study.

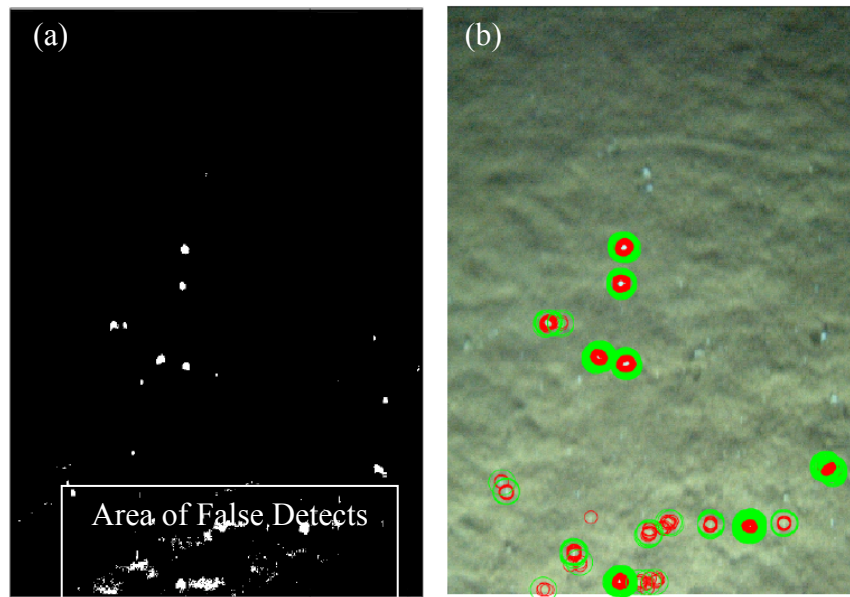


Figure 6: (a) Color detection analysis of a single image frame with a calibrated threshold for white; area of false detects resulting from proximity to strobe as indicated; (b) histogram analysis of same image showing detects based on mode ('Mode Detects' – green circles) and mean ('Mean Detects' – red circles).

The next step after calculating the number of detects for a given image was to calculate the areal coverage per frame of dead clam matter detections (those pixels that exceeded the 95% confidence interval in the histogram analysis). This was done by taking the vehicle altitude associated with each frame and then calculating the area associated with each pixel. This was then divided by the areal coverage of the frame to get the percentage coverage. Although this strategy was successful, there were a number of limitations including: (1) no detects in background; (2) manual screening of images; (3) no direct live clam detection; and, (4) false detects of debris and rocks.

No Detects in Background: There is a bias to detect clams in the foreground of the image as compared to the background. This is demonstrated in Figure 6b that clearly shows clams in the background that are not detected. Unfortunately, this is something that is not easily corrected as this is an artifact of physical arrangement of the strobe on the vehicle that is separated from the camera by ~ 1.5 m and so tends to light up the foreground to a greater extent than the background.

Manual Screening of Images: Before the algorithm could be applied, all of the images needed to be manually screened as sometimes the vehicle would be out of visual range of the bottom or the images would be so unfocused that they would be unusable. Given the number of images, this was quite time intensive and it is recommended that it be automated for future projects.

No Direct Live Clam Detection: This method only works for the detection of dead clam matter rather than the determination of live clam presence. To determine whether the relationship between the live and dead clams is constant around the lake can only be done using time intensive field techniques. It is also unclear whether dead clam matter remains *in situ* when it dies or if undergoes physical transport. This is something that is currently under investigation.

False Detects of Debris and Rocks: Although the program worked well for eliminating the false detects of large objects (i.e. boat anchors, large rocks, etc.) it wasn't able to discriminate small rocks and human debris (i.e. golf balls, aluminum cans, etc.). It was therefore necessary to "image truth" those areas with potential Asian clam detects and then to ground truth them using diving and sediment sampling techniques. Image truthing involved visually observing each image collected in all missions and was carried out over a four-month period by UCD and UNR staff as well as UBC researchers. Image truthing was necessary to narrow the amount of ground truthing necessary to confirm AUV detections (see Section 3.2).

2.4 *Algorithm Calibration*

Although the detection of dead clam matter from *UBC-Gavia* images is based on the detection of white pixels, it is the number of live clams that is of primary interest. Therefore, it was necessary to do a calibration between live clams and detections from the *UBC-Gavia* images. The basis of this calibration was the assumption that the ratio is constant throughout the lake and, in particular, along the south shore where both the known live clam communities and large piles of dead clam matter exist. Benthic grab samples were collected along a series of locations and then compared with the collected results from the images (Figure 7). Although there is variability in the results, the R^2 value is 0.66, $p = 0.10$, which

shows that there is a moderate agreement between the live clam populations and the image detections. The error bars at each data point represent a single standard deviation of different sample populations depending on the site. Large error bars reflect a more heterogeneous clam distribution within the boundaries of the field sampling area.

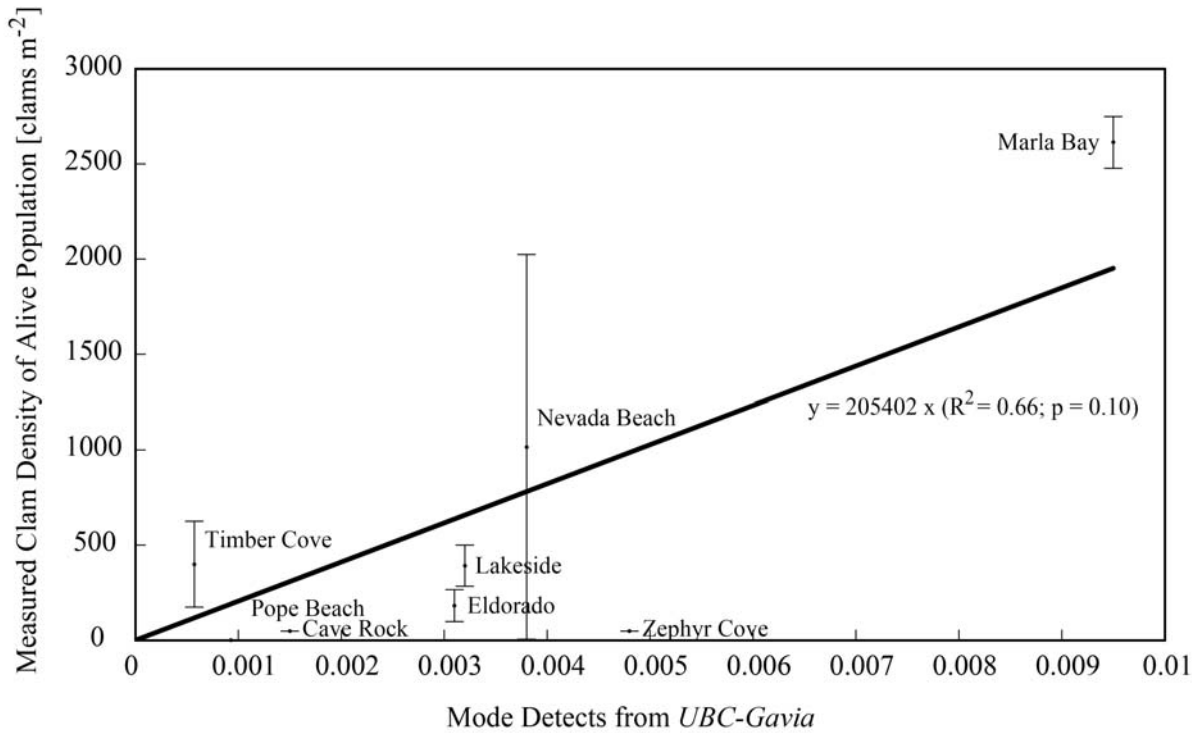


Figure 7: Calibration with PONAR grab samples (n=30) with error bars representing one standard deviation with varying sample populations: Timber Cove, Pope Beach, Cave Rock, Eldorado, Lakeside, Nevada Beach, Zephyr Cove, and Marla Bay.

3.0 Detection Results

After the initial manual filtering of the images, the algorithm was run and the raw data was plotted for different sections of the lake. It should be noted that a high pass filter was run on the processed data to eliminate the high false positives by removing data points above a certain threshold. The collected results were then used to make a map of the lake that highlighted

regions that could be returned to in a ground truthing campaign. A final map was then produced that combined the raw data and the ground truthed results.

3.1 Raw Data Results

Figure 8 through figure 19 show the Mode Detects normalized by bottom surface area for each section in the lake during the contour based missions. An inset is provided in each of the plots to show the location and a plan view representation of the data. In each of these insets, values below a threshold of 0.008 are shown in blue, 0.008 – 0.018 are shown in yellow, and greater than 0.018 are shown in red. These thresholds were determined mainly by trial and error to properly represent the known previously established, through scuba and diver surveys, clam distributions from Nevada Beach to Zephyr Cove. In addition, the high pass filter value of 0.02 was selected by trial and error by examining images with known debris or rock detections. The reported Mode Detects from these frames were then used to establish the high threshold. The plotted along track distance is from the initial point of each track (shown with the star in each inset) to the final point of each track (shown with the square in each inset) as shown along the x-axis in each image. It should also be noted, that there was significant variability at any given location as a result of the many images collected at each location (collected at a frequency of 4 Hz). This is clearly demonstrated in Figures 8 through 19 and particularly prevalent in regions of high clam density (e.g. Marla Bay – Figure 8). This was partially the result of the variability of dead clam matter in each image and light conditions in each frame. Overall it is the trends in the data that are important to observe.

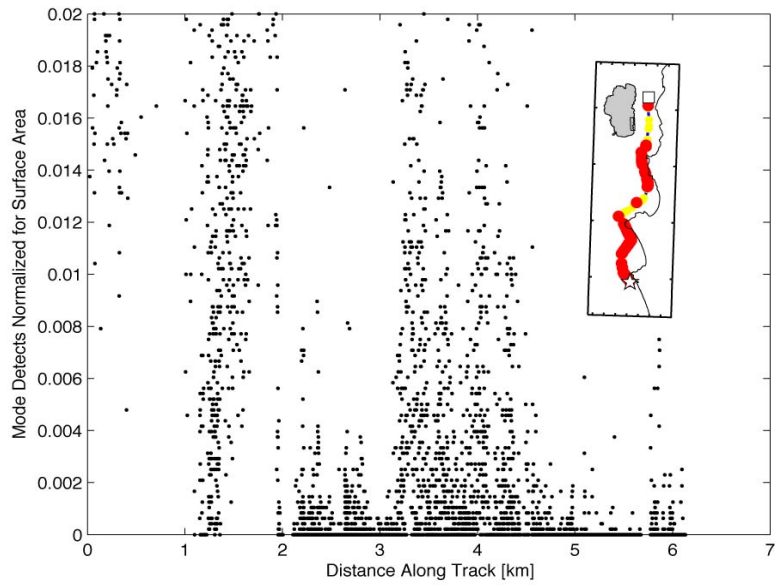


Figure 8: Processed image data from the area from Marla Bay past Zephyr Cove.

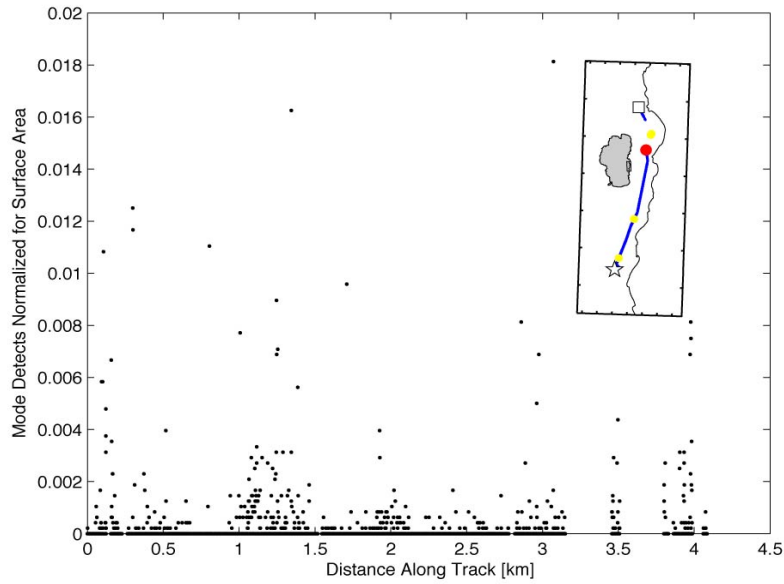


Figure 9: Processed image data from the area from Cave Rock to Glenbrook.

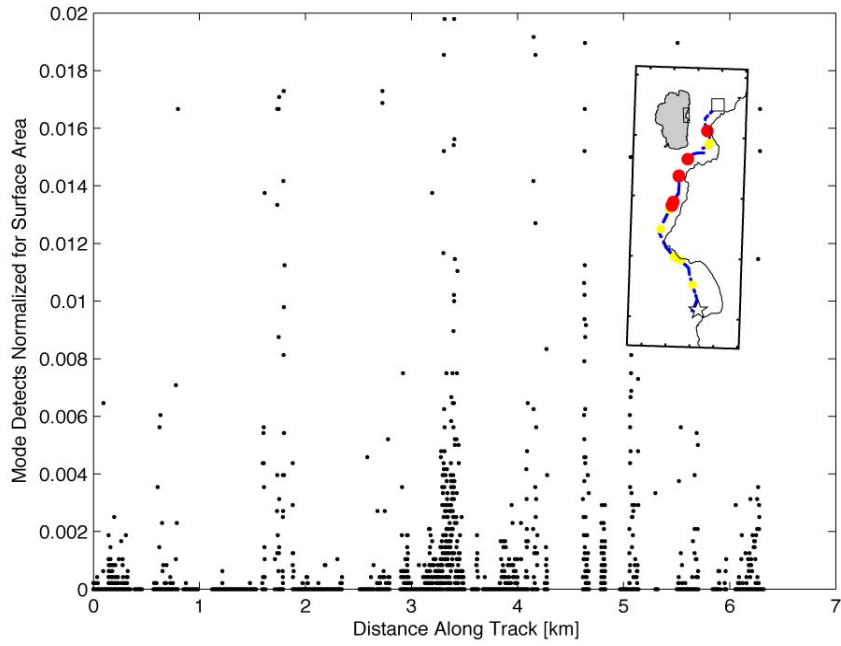


Figure 10: Processed image data from the area from north of Glenbrook.

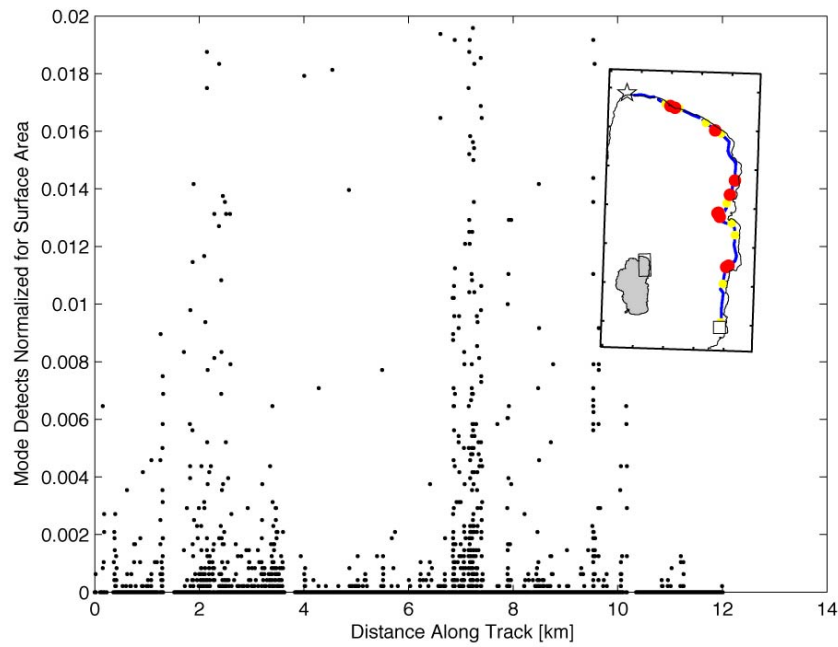


Figure 11: Processed image data from the area from Incline Village to Sand Harbor.

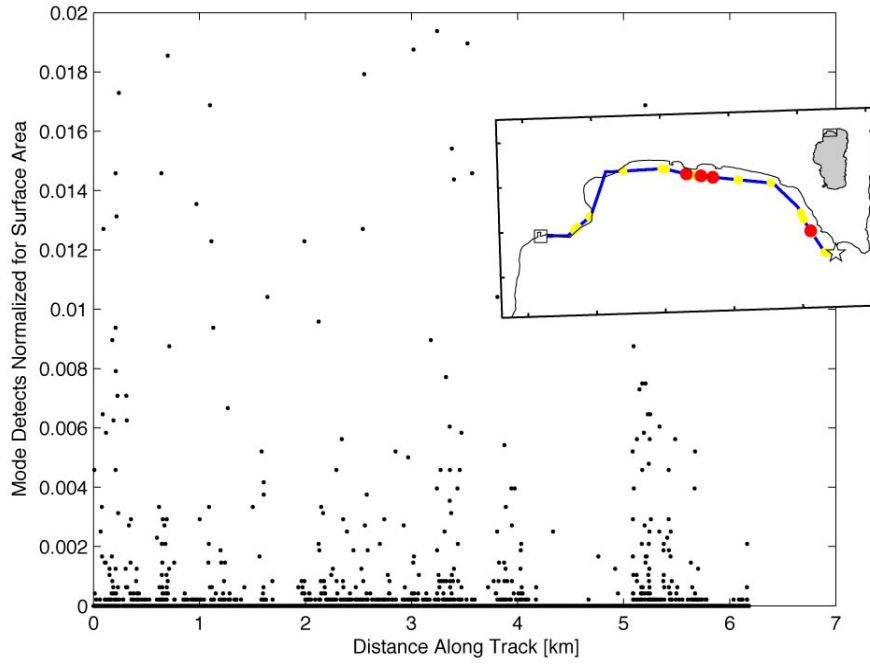


Figure 12. Processed image data from the area from King's Beach to Tahoe City.

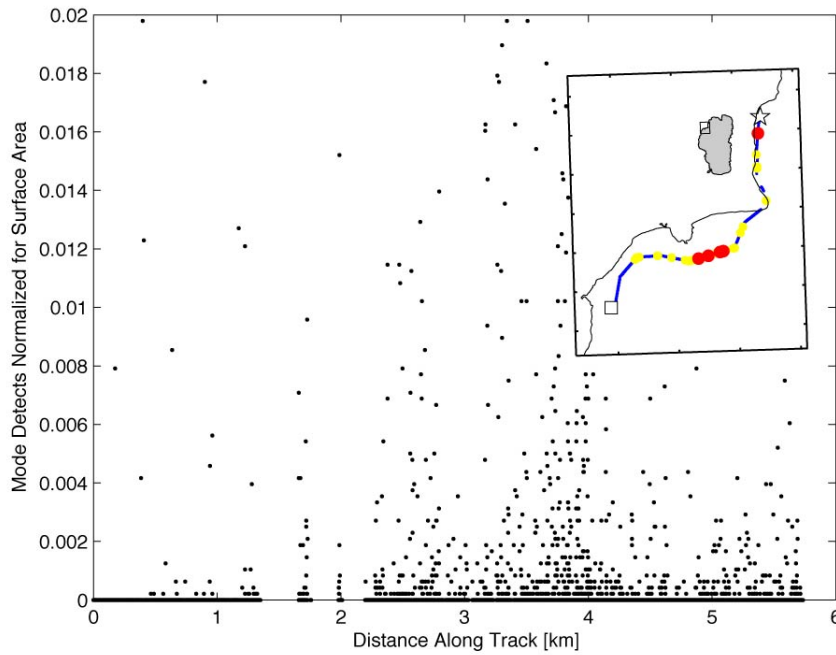


Figure 13: Processed image data from the area from Tahoe City to the Truckee River.

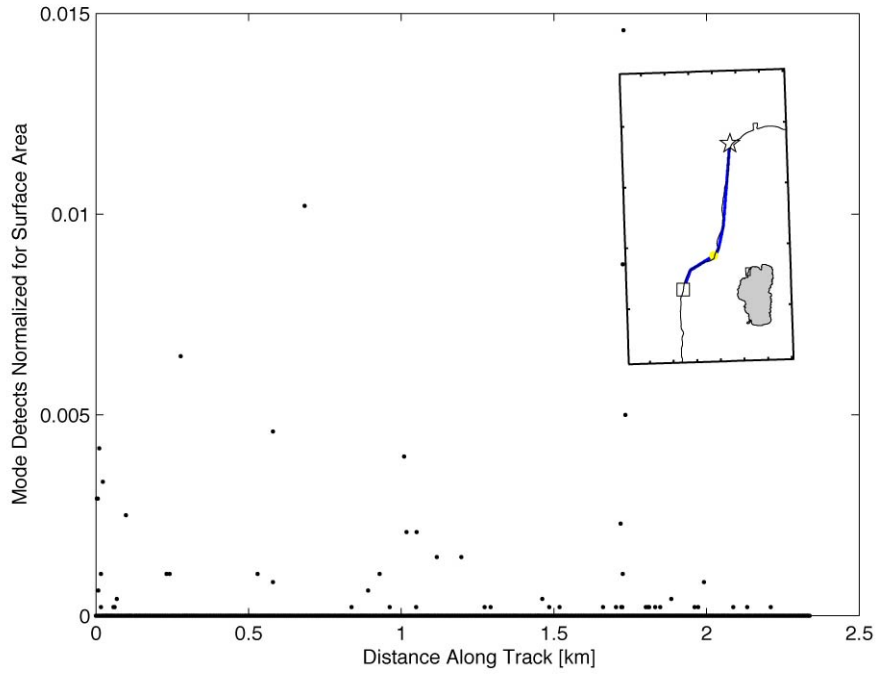


Figure 14: Processed image data from the Tahoe City shelf.

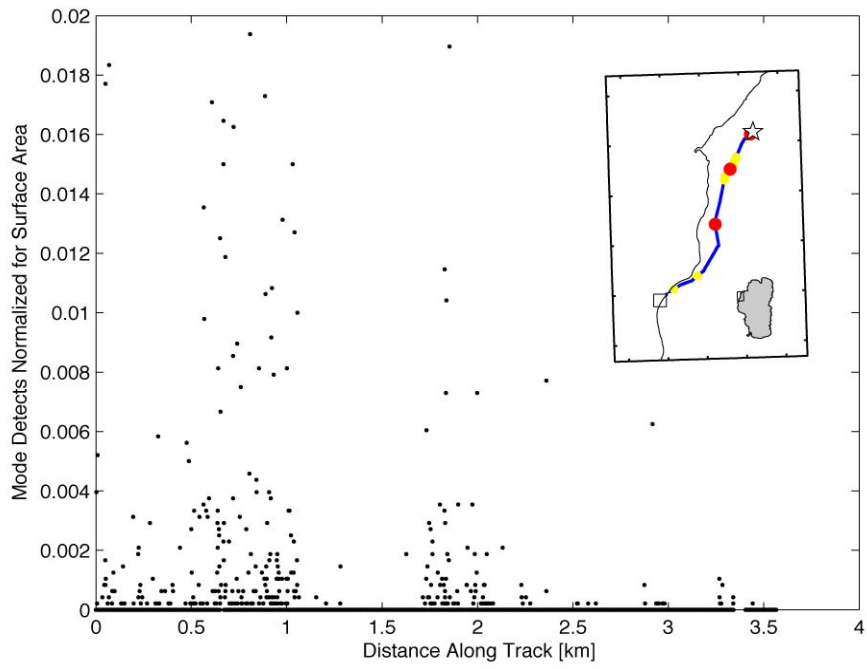


Figure 15: Processed image data from Tahoe City to Homewood.

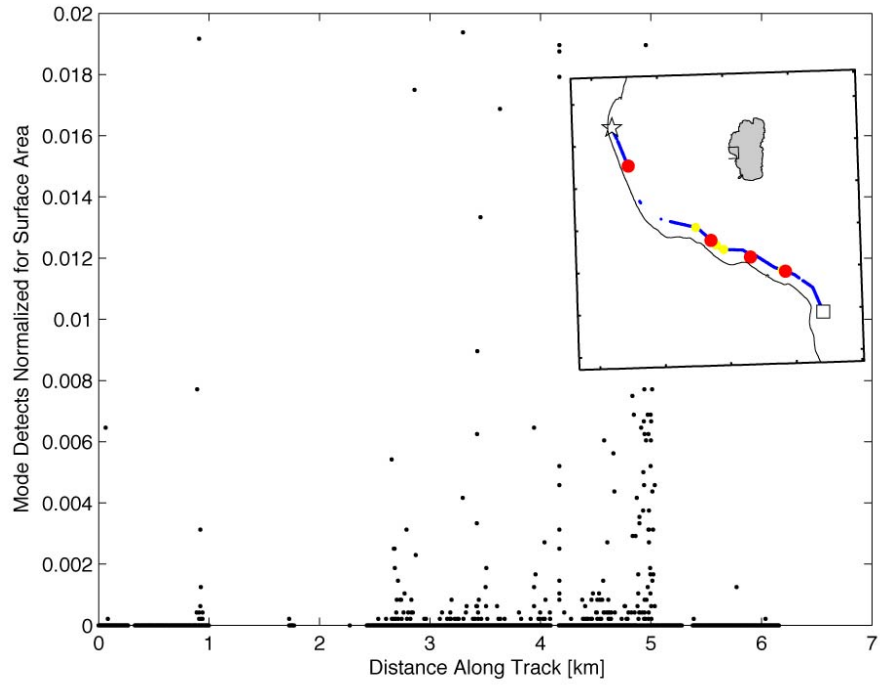


Figure 16: Processed image data from the area from Homewood to Sugar Pine Point.

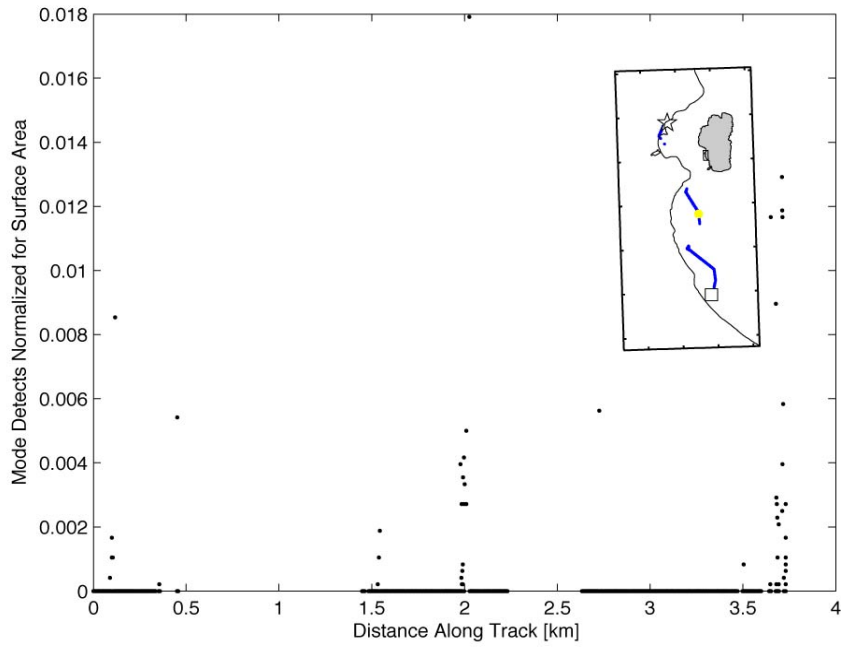


Figure 17: Processed image data from the area from Meeks Bay to Rubicon Point.

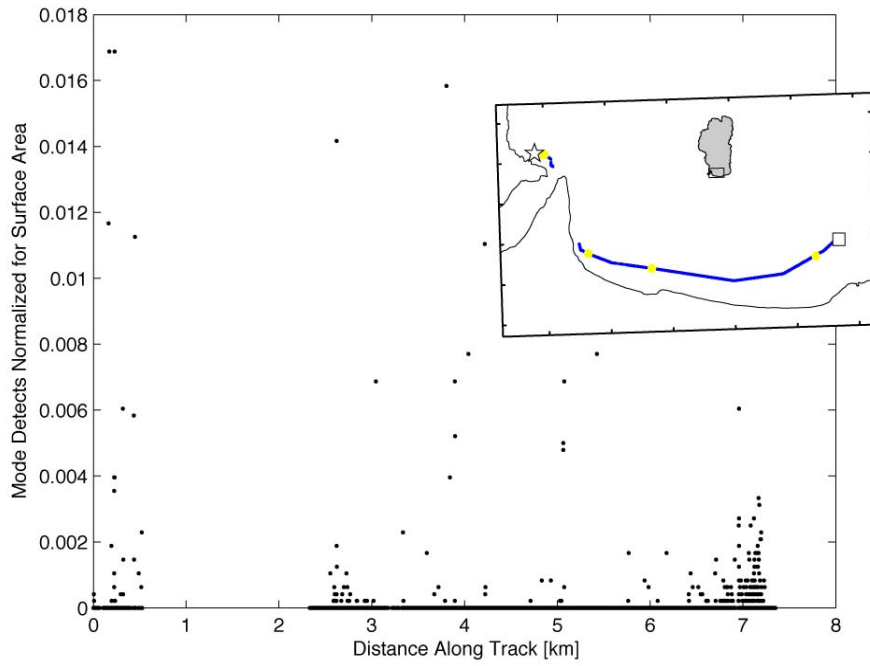


Figure 18. Processed image data from the area from Emerald Bay to Tahoe Keys.

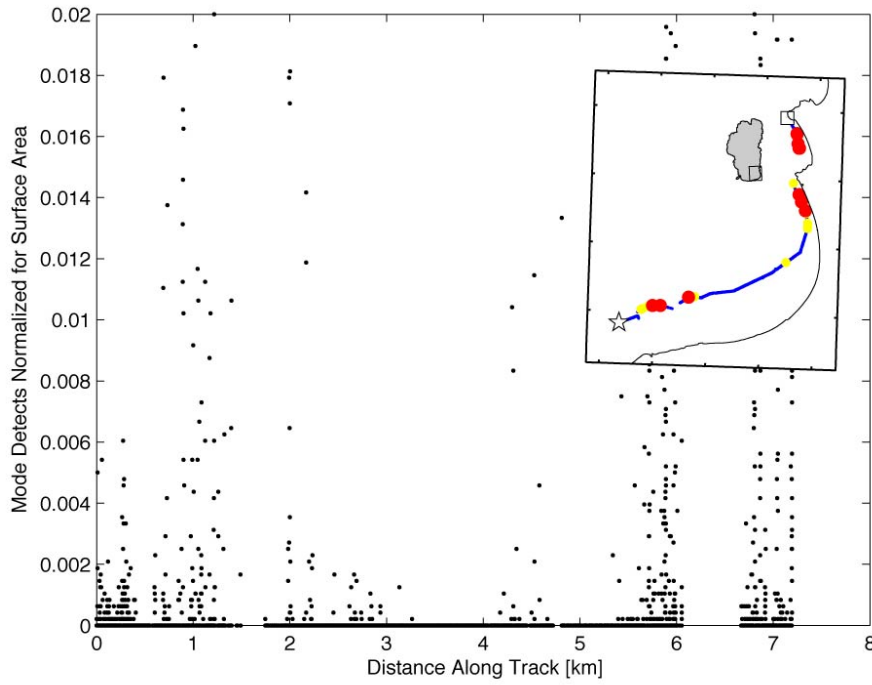


Figure 19: Processed image data from the area from Tahoe Keys to Marla Bay.

3.2 *Groundtruth Surveys*

Combining all of these results, it is possible to create a single map (Figure 20a) that shows those regions, in orange, that the AUV imagery indicates potential presence of dead clam shell matter. In total, the results show nine potential regions at various locations around the lake that required confirmation. These sites were investigated using divers in a groundtruth campaign that took place from August 2009 through May 2010. In all, only two of the nine sites where AUV imagery indicated the potential presence of clams were found to support clams were (1) near the Tahoe Keys (south), and (2) near Incline Village (northeast) (Figure 20b). Of these two, the site on the south shore proved positive for the presence of Asian clam (indicated in red). The north shore site (indicated in green) proved negative for Asian clam but did show presence of *Pisidium* (a smaller native species of clam resident in Lake Tahoe).

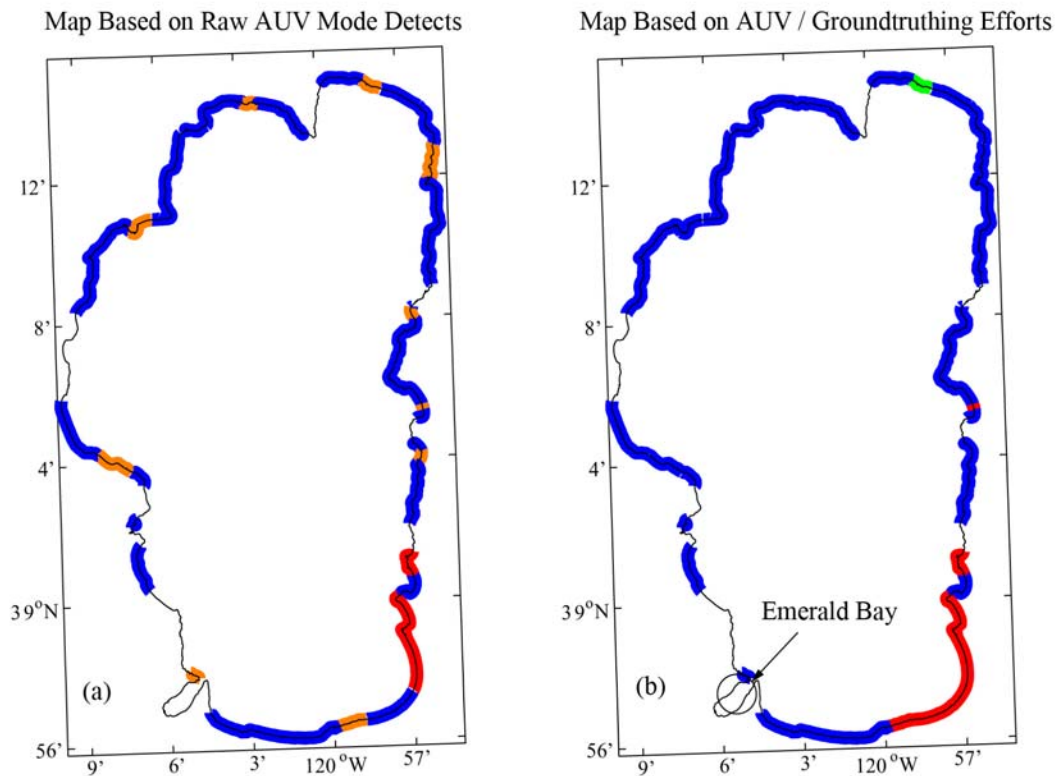


Figure 20: Map of clam distribution in Lake Tahoe from (a) AUV raw data, and (b) after the groundtruthing campaign.

In general, the rest of the sites that suggested the possibility of clam populations turned out to be a series of false positives resulting from high concentrations of mica and white gravel mixed in amongst darker gravel in the lake bottom. Contour following missions were not run in those regions of the lake with no color associated with the shoreline because of habitat unsuitability (i.e., sheer walls, boulder substrate). The large region along the west shore near Homewood was not run due to the fact that the vehicle got trapped on the bottom and had to be retrieved by divers. It was intended to return to this area at the end of the study, but this was decided against due to a mechanical failure on the main drive shaft of the vehicle on the last night of deployment. The only additional region that was not explored was within Emerald Bay itself. A detailed SCUBA survey for Asian clam was conducted during September and October 2009, after the

AUV survey was conducted. This survey showed that live Asian clam populations with densities that range from 30 – 100 individuals/m² are present in a 0.75 km² area in the mouth of Emerald Bay (at Eagle Point). This survey will be repeated in September 2010.

3.3 Across Shore Transects

After the 5 m contour along-shore transects were completed, several sites were selected for across-shore or inshore-offshore transects. That is, surveys were run perpendicular to shore to examine the variability of the clam distribution with depth. These sites included Baldwin Beach, Camp Richardson, Eldorado Beach, Marla Bay, Nevada Beach, Tahoe Keys, and Timber Cove (all but the first two sites shown in Figure 1). Missions were designed to run from roughly 2 – 80 m depth. Of these sites, image detects were made in Marla Bay, Nevada Beach and Timber Cove and, of these three, only the first two had full vertical profiles collected with PONAR grab samples. Using the relationship developed in Figure 7 (density [clam m⁻²] = 205402 image_detects), it is possible to convert the image detections at each depth to live clam densities (Figure 21 and Figure 22). The image detections in each of these plots have been bin-averaged at 1 m intervals and then the PONAR grab sample results have been overlain. In Figure 21, when the grab samples are displaying non-zero results, it was shown that the two sampling techniques are in relatively close agreement although the point sampling technique shows a much higher degree of variability than the image detections; either showing density values of 0 or a value <2000 clams m⁻². This is a result of the results for the image detections being averaged together as there was also a large portion of zero detection for each bin average. It should also be noted that point sampling only continued to a depth of ~ 27 m whereas image results were collected down to a depth of 40 m and suggest significant populations at these deeper depths.

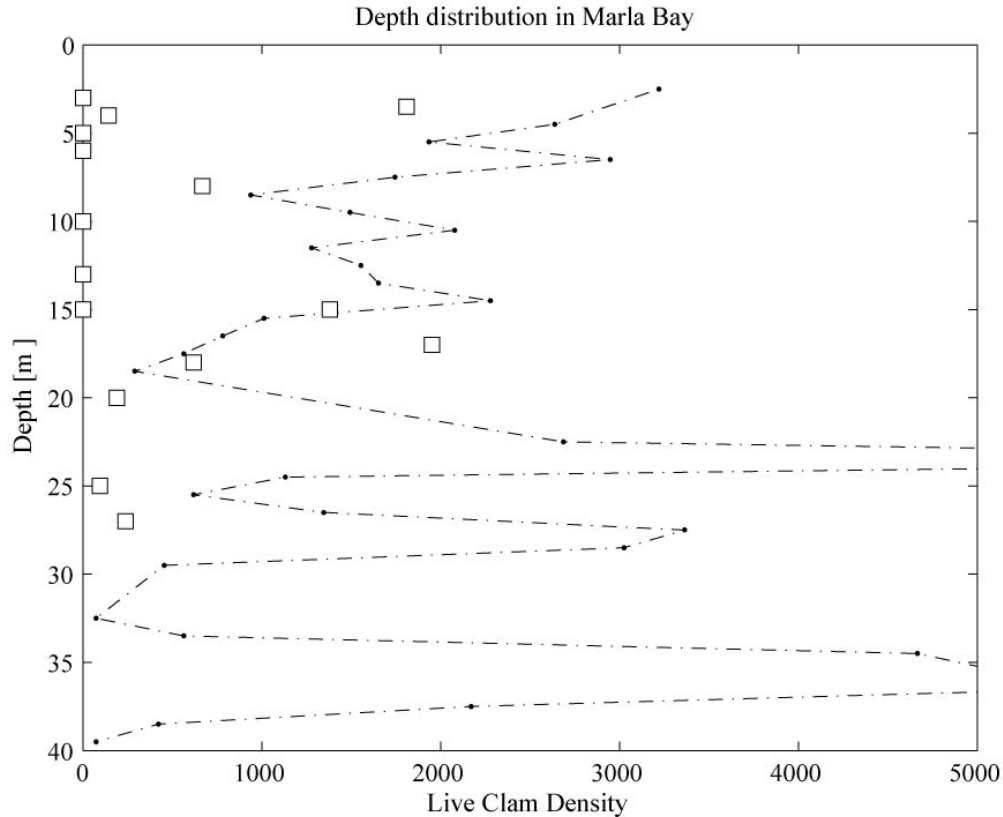


Figure 21: Depth profile generated from across-shore transect results at Marla Bay with calculated clam data based on 1 m bin-averaged image detection results (dash dot line) and single point PONAR grab samples with actual results (open faced squares).

Unfortunately, there's much less agreement in the profile taken from Nevada Beach as a result of the fact that the bulk of the PONAR samples were taken at depths less than 20 m while the image detections were generally measured below this depth (Figure 22). This is mainly the result of the very steep slopes in the 10 – 20 m region of the slope that prevented good quality images from being collected at these depths. Below the 20 m depth there is close agreement with the PONAR results with image detection results although these are all quite low values.

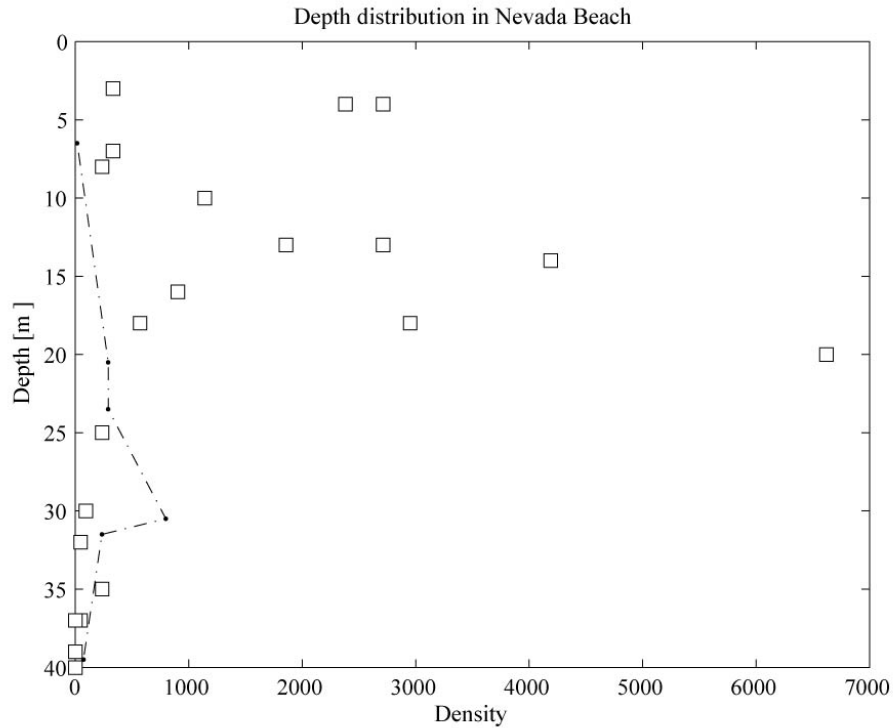


Figure 22. Depth profile generated from across-shore transect results at Nevada Beach with calculated clam data based on 1 m bin-averaged image detection results (dash dot line) and single point PONAR grab samples (open faced squares).

4.0 Water Column Parameters

4.1 Temperature and Conductivity Results

Part of the scientific payload of the AUV was a Seabird 49 Conductivity-Temperature-Depth (CTD) profiler that samples at these three parameters at 16 Hz. One of the working theories was that regions of clam growth (e.g. Marla Bay) would have slightly different water column characteristics than the rest of the lake (e.g. warmer or saltier). To explore this, it is necessary to measure the background stratification and in order to compare the measured results with this. While AUV missions were being run, concurrent vertical profiles were being collected from the boat with a Seabird 19plus CTD. In total, five different profiles were gathered along the south

shore to depths of 7 – 100 m. Taking the 1 m bin-average of the temperature results, it is possible to delineate the three regions in the water column known as the epilimnion, metalimnion, and hypolimnion (Figure 23). Most of the contour missions were run in the epilimnion region although there were sometimes depth excursions to deeper depths, while the across-shore transects spanned all three of these regions. The short temperature deviations around 7 m are an artifact of average all of the results together.

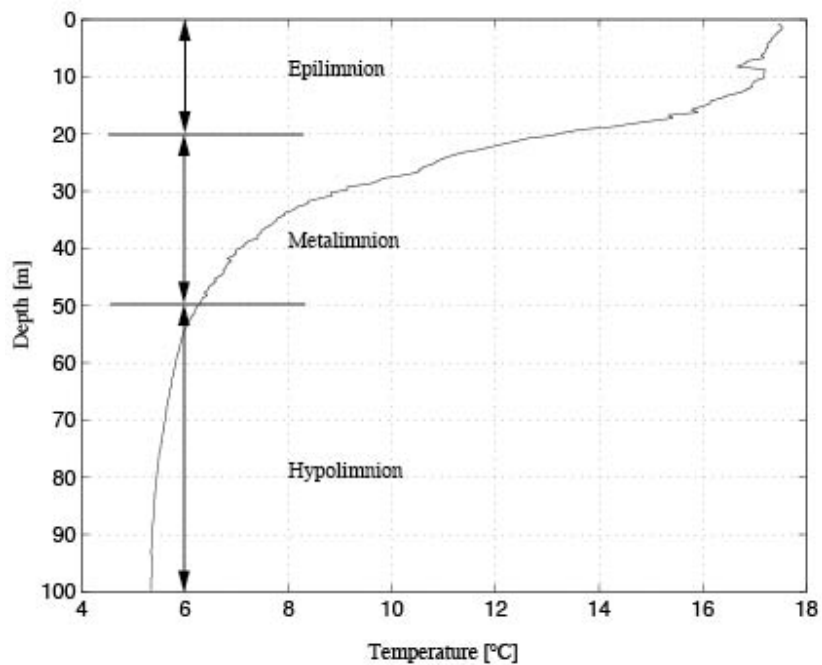


Figure 23: 1 m bin-averaged results of the temperature measurements of the background stratification of the lake taken in August, 2009 with the three thermal regions of the lake delineated; epilimnion, metalimnion, and hypolimnion.

As these were measured on different days and relative times, there will be differences in measured temperatures and conductivities and so it is necessary to standardize the results to a common reference frame. The approach taken to do this was to plot temperature versus specific conductivity in a similar fashion to temperature versus salinity plots that are commonly used in oceanography to characterize different water masses. It should be noted that specific

conductivity, conductivity corrected to a reference temperature, is more commonly used in freshwater systems with low conductivities ($< 1000 \mu\text{S cm}^{-1}$), which Lake Tahoe ($\sim 25 \mu\text{S cm}^{-1}$) satisfies, than salinity. The results of this analysis for the vertical casts are shown in Figure 24 that is interpreted to show two water masses; one warmer with a slightly higher specific conductivity associated with the epilimnion and the other cooler with a slightly lower specific conductivity. Values between these two end members represent some mixture of these two water masses. Although there are several possible reasons for the slightly higher conductivity signal in the epilimnetic waters, the most likely is increased evaporation rates at the surface as compared to the deeper waters.

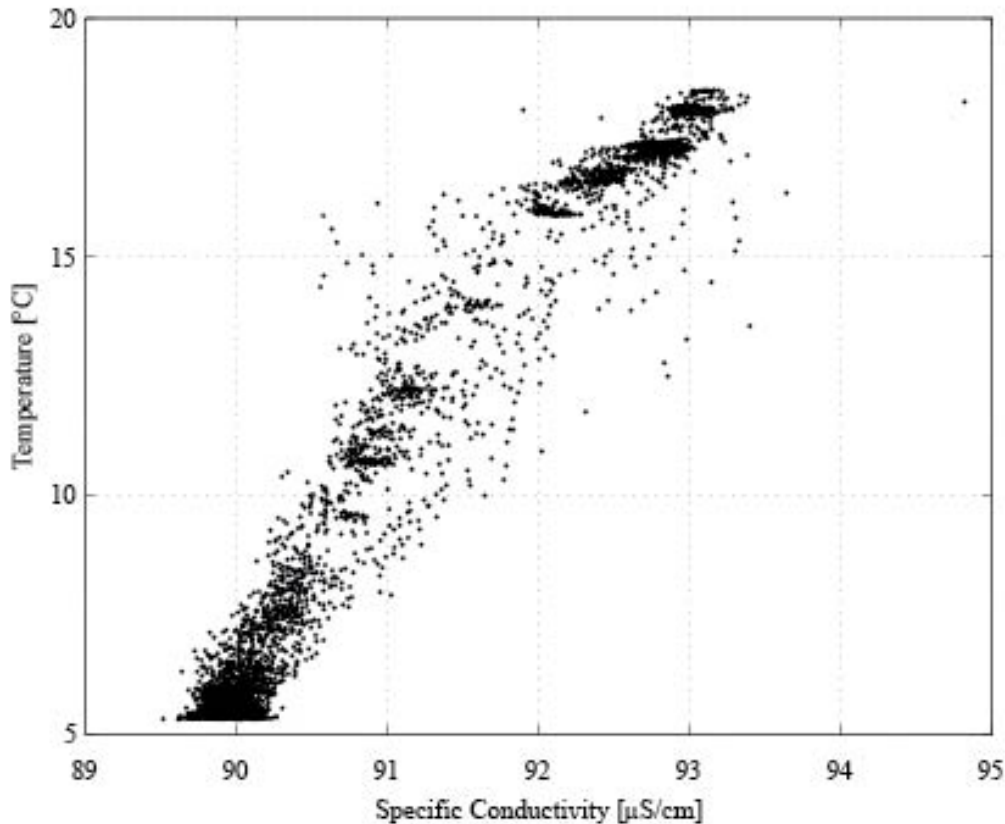


Figure 24: Temperature versus specific conductivity plot of the ambient conditions measured last summer during the AUV campaign.

The next step would have been to then overplot each of the deployments to see if there were any additional characteristic water masses and then identified where those were. Unfortunately, the conductivity values being recorded from the AUV were extremely variable which would indicate a potential problem with the sensor and so it was not possible to use this data. However, the temperature values recorded by the AUV closely matched the profile shown in Figure 23 and displayed no indication to suggest additional water types. Although a more detailed study would be required to characterize this further, there is currently no evidence from this work to suggest that different areas have different water types.

4.2 Chlorophyll a, CDOM and Turbidity Results

As previously mentioned, *UBC-Gavia* was equipped with a three-channel fluorescence and light scattering unit, a Wetlabs™ BB3 Ecopuck, that chlorophyll-*a*, CDOM and turbidity can be derived from. The BB3 collects single-wavelength measurements of chlorophyll-*a* by directly measuring the amount of chlorophyll-*a* fluorescence emission from a given sample volume of water in a similar way that CDOM is measured on a separate channel. Turbidity was measured simultaneously by detecting the scattered light from a 700 nm LED at 140 degrees to the same detector used for fluorescence. The turbidity measurement was performed at the same 140 degree angle as the chlorophyll fluorescence.

Results for each parameter (depth, CDOM, turbidity and chl *a*) are presented in Table 1. On the left side of the table unfiltered results are presented (raw data collected by AUV) and on the right hand side, filtered results are presented.

	No filter, all data			Depth of AUV > 0.6m Altitude > 0.1m		
	Mean	Min	Max	Mean	Min	Max
Depth of AUV (m)	8.44	-0.32	120.64	16.22	0.60	120.64
Altitude between AUV and bottom (m)	4.32	0	43.64	4.41	0.10	42.14
Total depth (m)	12.76	-0.32	132.74	20.64	2.60	132.74
CDOM (ppb)	15.39	-4.60	344.43	0.95	0.25	3.01
Turbidity ($\text{m}^{-1} \text{sr}^{-1}$)	0.0024	-0.0001	0.0130	0.0004	0.0002	0.0085
Chlorophyll ($\mu\text{g/l}$)	1.29	-0.55	49.72	0.32	0.037	1.85

Table 1: Statistics for each filter and filtering influence

CDOM, chl-*a* and turbidity showed no close correlation with AUV imagery results. Figure 25 shows the ‘hot spot’ locations (elevated results) and in all other areas in the lake were below the mean detection limit of the Ecopuck detection limits. These results are comparable with other pristine lakes. Elevations in CDOM concentrations are present in front of the Truckee River inflow along the south shore and also at Elk Point and South Marla Bay on the southeast shore. Elevated concentrations of chl *a* are present at the northern Incline Village site as well as near Kings Beach, east of Brockway Point. Finally, increases in turbidity are noticeable at two sites along the west shore (Figure 25).



Figure 25. Detail of Lake Tahoe showing results of the optical backscatter channels with areas of relatively high intensity of each component (chlorophyll-*a*, turbidity and CDOM) at the 5 m lake contour.

Figure 26 shows vertical profiles of CDOM, chl-*a* and turbidity from all of the across shore profile sites along the southeast shoreline and filtered at a constant altitude of 2.6 m from the bottom. Although fairly uniform with depth, there does appear to be a slight increase in chl-*a* at ~40 m which corresponds with the depth of chlorophyll maximum for this time of the year. Discretization observed in the CDOM profile results is thought to result from instrument

resolution at measured values this close to the detection limit. The turbidity profile shows three layers at roughly 2, 10 and 20 m that show departures from the mean, albeit quite low values.

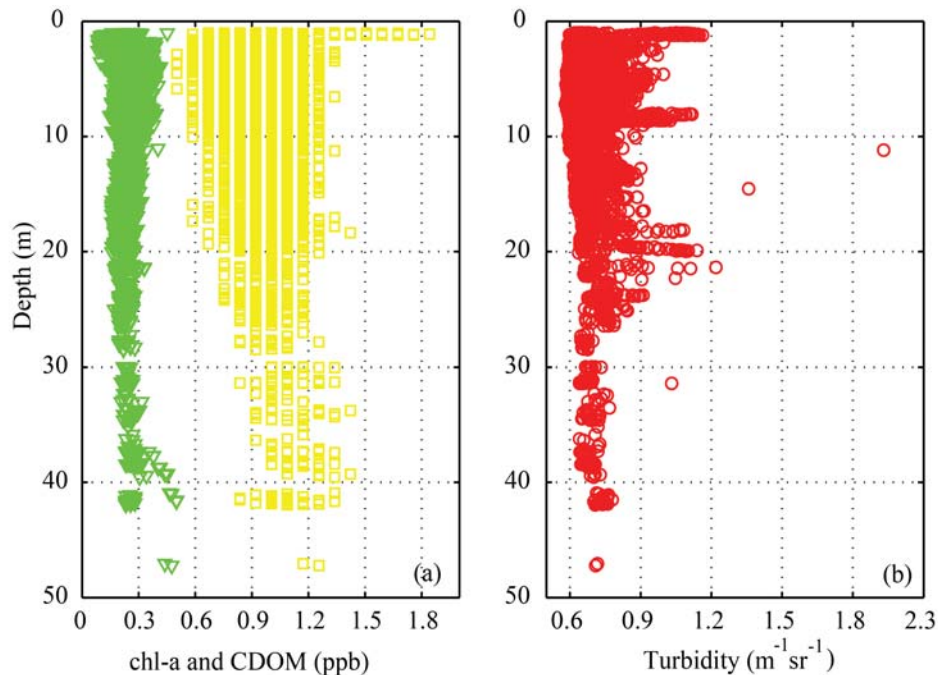


Figure 26, Vertical profiles of chl-*a* (green), CDOM (yellow) and turbidity (red) from all of the across profile sites along the southeast shore.

5.0 Correlation between filamentous algae and Asian clam presence

There are a limited number of studies that suggest that filter feeding invasive bilalves can alter nutrient cycling to promote the growth of filamentous algal species such as *Cladophora glomerata* (Hecky et al., 2004, Higgins 2005). The presence of high density populations of these species, filter feeding and shifting phosphorus cycling leads to alterations to primary productivity in areas immediate to invasive bivalve habitat. Laboratory bioassay studies conducted by UC Davis Tahoe Environmental Research Center showed that the addition of Asian clam excretory material to pelagic and filamentous algal species resulted in an increase in algal growth over a 10 day period (Wittmann et al. 2008, Wittmann et al. forthcoming). In 2008 – 2010 in Lake Tahoe,

there were dense blooms of filamentous algal species associated with Asian clam populations. In order to further understand the relationship between observed filamentous algal biomass (*Zygnema sp.*, *Spirogyra sp.*, *Cladophora glomerata* and other species) and Asian clam presence, *UBC-Gavia* images were analyzed for the co-occurrence of these algal and molluscan taxa. To do so, 5% of images from each mission run (N = 40 to 450) were randomly selected (using random number generation on directories of image files) and visually assessed for the collocation of filamentous algae and Asian clam. Of the total number of images assessed (N = 3090), 8.9% (N = 274) contained clams, and 4.4% (N = 137) contained filamentous algae. Of the images that contained Asian clam, 47.8% contained filamentous algae, and of the images that contained filamentous algae, 95.6% contained Asian clam. To summarize the relationship of the entire lakewide co-location of these taxa, we calculated a Phi coefficient of correlation (analogous to a Pearson coefficient of correlation but for binomial terms, i.e., presence/absence) between algal and clam presence in image samples. The Phi coefficient for this observed relationship is -0.15, which suggests that on a lakewide level, there is little to no correlation between filamentous algal growth and Asian clam presence. This could be explained by the observation of filamentous algae in areas where there are no Asian clams such as Crystal Bay and other regions on the west shore such as Tahoe City where algal growth was observed. And conversely, multiple observations of Asian clam (52.2% of images) with no algal growth observed. Further, we examined the relationship between *C. fluminea* population density and filamentous algae co-occurrence with depth to understand whether there was a population threshold for which Asian clam might have an impact on filamentous algae presence. This analysis showed a general occurrence of algae in 5 – 7 m water depth (which is the general zone where *UBC-Gavia*

travelled), and no significant trend between algal presence and *C. fluminea* population densities (Figure 27).

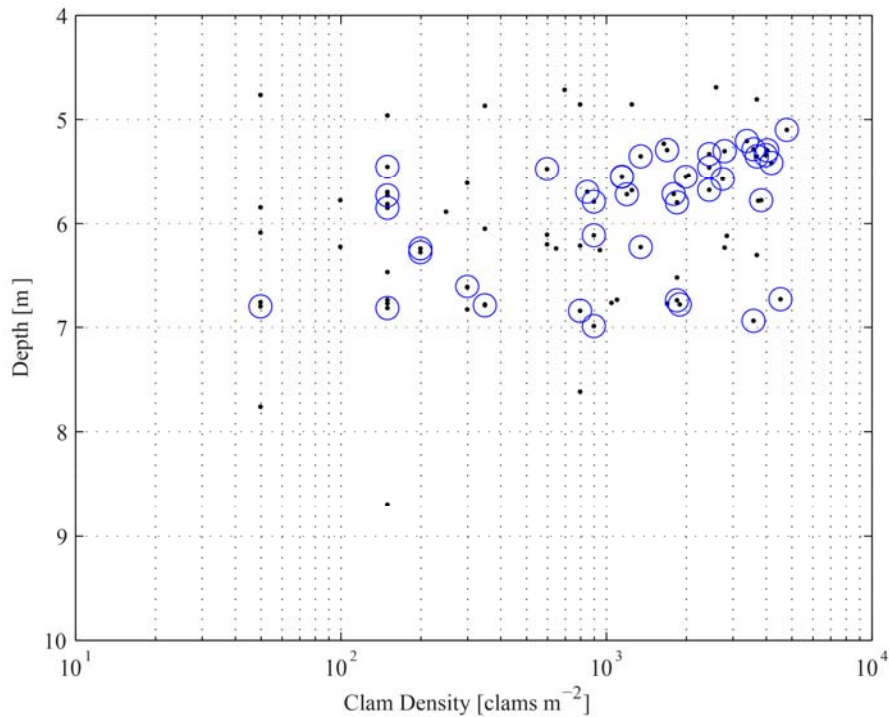


Figure 27. Bivariate plot showing the co-location of Asian clam population density (black dots) with depth and the presence of filamentous algae (blue circles).

Both Figure 27 and the low Φ -correlation coefficient suggest that there are more factors contributing to algal occurrence than *C. fluminea* presence alone. In general, localized sites identified as positive for algal growth have been identified as urban areas (Incline Village, Tahoe City), areas of high nutrient creek input (Incline Village), or areas of occurrence of *C. fluminea* in high densities (Marla Bay, Zephyr Cove, Nevada Beach). So it is likely to assume that there is an ecological correlation between nutrient output by *C. fluminea* and the occurrence of filamentous algae under field conditions, but that *C. fluminea* is not the sole explanatory variable in filamentous algae presence in Lake Tahoe. This analysis is limited in that the highest densities

of filamentous algal growth observed in the field have occurred in shallower waters (1 – 4 m in the Round Hill Pines Marina Cove, Timber Cove and near Regan Beach) where surveys with *UBC-Gavia* were not conducted because of water depth limitations. To gain more certainty about this relationship, further research must be conducted in shallower waters of the littoral zone.

6.0 Other observations

Analysis of *Gavia* imagery provided some further insight to the distribution of other taxa in Lake Tahoe's littoral zone. Aquatic macrophytes were very infrequently detected with the AUV survey because most macrophyte species are present at water depths < 5 m and within marinas. The *Gavia*'s course was restricted to deeper water depths to target the likelihood of observed Asian clam beds. However, large beds of *Chara* were observed in the southwestern portion of the lake (near Camp Richardson/Pope Beach area) at 15 – 20 m water depth.

7.0 Conclusions

The following are the conclusions from this research:

- Asian clam are generally detected in the southeastern quadrant of the lake.
- Highest densities of Asian clam are detected in Marla Bay.
- Asian clam are not present north of Emerald Bay on the West shore.
- Asian clam are not present north of Glenbrook Bay on the East shore.
- Asian clam are not present on the North shore.
- New populations of Asian clam were detected as a result of the AUV survey at water depths not previously surveyed (>50 m in Marla Bay, Nevada Beach, and near the Tahoe Keys).

- There is a correlation between the number of Asian clam shells on the sediment surface as detected by Gavia detects and live Asian clam population densities ($R^2 = 0.66$, $p = 0.10$).
- A scuba survey showed that there are live Asian clam populations in Emerald Bay at Eagle Point. This survey will be repeated in September 2010.
- There are elevations in turbidity at two sites in McKinney Bay on the West shore.
- There are elevations in CDOM concentrations at the Truckee River Inflow and at Elks Point.
- There are detected elevations in chl-*a* near Kings Beach and Incline Village.
- Approximately 96% of the observations of filamentous algae, there are Asian clam present. In 48% of the observations of Asian clam, there are filamentous algae present. On a lakewide level, there is little to no correlation (Phi coefficient = -0.15) between the presence of filamentous algae and Asian clam. This analysis suggests that filamentous algal growth is highly correlated with Asian clam presence, but that there are other factors/nutrient inputs that can contribute to the presence of filamentous algal growth. Further research is needed.

8.0 Acknowledgements

We would like to acknowledge the Lahontan Regional Water Quality Control Board for securing funding for this endeavor from the State Water Resource Control Board Clean Up and Abatement Fund and Nevada Division of State Lands for funding the ground-truthing portion of this project. The US Fish and Wildlife Service and the Tahoe Regional Planning Agency have provided ancillary funds and support for other components of Asian clam surveying, research and management. We would like to thank all the participants in the AUV survey for supporting the deployment and analysis of this work.

9.0 References

- Hecky, R.E., R. EH Smith, D. R. Barton, S. J. Guildford, W. D. Taylor, M. N. Charlton, and T. Howell. 2004. The nearshore phosphorus shunt: a consequence of ecosystem engineering by dreissenids in the Laurentian Great Lakes. *Can. J. Fish. Aquat. Sci.* 61(7): 1285–1293.
- Higgins, S. N. 2005. Modeling the growth dynamics of *Cladophora* in eastern Lake Erie. Ph.D. Thesis, University of Waterloo, Waterloo, Ontario, 153p.
- Wittmann, M.E., Reuter, J.E., Schladow, S.G., Hackley, S., Allen, B.C., Chandra, S., Caires, A. 2008. Asian clam (*Corbicula fluminea*) of Lake Tahoe: Preliminary scientific findings in support of a management plan.
Online: <http://terc.ucdavis.edu/research/AsianClam2009.pdf>